Hauser, S.; Wodtke, R.; Tondera, C.; Wodtke , J.; Neffe, A.; Hampe, J.; Lendlein, A.; Löser, R.; Pietzsch, J.:
Characterization of Tissue Transglutaminase as a Potential Biomarker for Tissue Response toward Biomaterials.
In: ACS Biomaterials Science & Engineering. Vol. 5 (2019) 11, 5979 - 5989.
First published online by ACS: 07.10.2019

DOI: 10.1021/acsbiomaterials.9b01299
https://dx.doi.org/10.1021/acsbiomaterials.9b01299

Characterization of Tissue Transglutaminase as potential Biomarker for Tissue Response towards Biomaterials

Sandra Hauser[1], Robert Wodtke[1], Christoph Tondera[2], Johanna Wodtke[1], Axel T. Neffe[3, 5,#], Jochen Hampe[4], Andreas Lendlein[3, 5, 6], Reik Löser[1,7], Jens Pietzsch[1,7*]

[1]Institute of Radiopharmaceutical Cancer Research, Helmholtz Center Dresden-Rossendorf, Dresden, Germany

[2]Biotechnology Center (BIOTEC), Center for Molecular and Cellular Bioengineering (CMCB), Technical University Dresden, Dresden, Germany

[3]Helmholtz Virtual Institute on Multifunctional Biomaterials for Medicine, Teltow, Germany

[4]Medical Department 1, University Hospital Dresden, Technical University Dresden, Dresden, Germany

[5]Institute of Biomaterial Science and Berlin-Brandenburg Center for Regenerative Therapies (BCRT), Teltow, Germany

[6]Institute of Chemistry, University of Potsdam, Potsdam, Germany

[7]Faculty of Chemistry and Food Chemistry, School of Sciences, Technical University Dresden, Dresden, Germany

#: current address: Institute for Technical and Macromolecular Chemistry, University of Hamburg, Germany

*Corresponding author: Jens Pietzsch, j.pietzsch@hzdr.de, 0049 351 2602622

Abstract

Tissue transglutaminase (TGase 2) is proposed to be important for biomaterial-tissue interactions due to its presence and versatile functions in the extracellular environment. TGase 2 catalyzes the crosslinking of proteins through its Ca^{2+}-dependent acyltransferase activity. Moreover, it enhances the interactions between fibronectin and integrins, which in turn mediates the adhesion, migration and motility of the cells. TGase 2 is also a key player in the pathogenesis of fibrosis. In this study, we investigated whether TGase 2 is present at the biomaterial-tissue interface and might serve as an informative biomarker for the visualization of tissue response toward gelatin-based biomaterials. Two differently cross-linked hydrogels were used, which were obtained by the reaction of gelatin with lysine diisocyanate ethyl ester. The overall expression of TGase 2 by endothelial cells, macrophages, and granulocytes was partly influenced by contact to the hydrogels or their degradation products, although no clear correlation was evidenced. In contrast, the secretion of TGase 2 differed remarkably between the different cells, indicating that it might be involved in the cellular reaction toward gelatin-based hydrogels. The hydrogels were implanted subcutaneously in immunocompetent, hairless SKH1-Elite mice. *Ex vivo* immunohistochemical analysis of tissue sections over 112 days revealed enhanced expression of TGase 2 around the hydrogels, in particular at days 14 and 21 post-implantation. The incorporation of fluorescently labeled cadaverine derivatives for the detection of active TGase 2 was in accordance with the results of the expression analysis. The presence of an irreversible inhibitor of TGase 2 led to attenuated incorporation of the cadaverines, which verified the catalytic action of TGase 2. Our *in vitro* and *ex vivo* results verified TGase 2 as a potential biomarker for tissue response toward gelatin-based hydrogels. *In vivo*, no TGase 2 activity was detectable, which is mainly attributed to the unfavorable physicochemical properties of the cadaverine probe used.

Keywords

Extracellular matrix modifying enzymes; gelatin-based hydrogels; biomaterial-tissue interface; polyamines; optical imaging

Introduction

Tissue transglutaminase (TGase 2) is the most frequent member of the transglutaminase family and is important for biomaterial-cell or biomaterial-tissue interactions due to its presence and versatile functions in the intra- and extracellular environment [1-3]. Of particular importance is the Ca^{2+}-dependent acyltransferase activity via which TGase 2 catalyzes the formation of isopeptide bonds between a primary amine, such as a protein-bound lysine, and a protein-bound glutamine [4]. Thereby, a cross-link between or within proteins is formed, which enhances the stability of proteins toward degradation. In addition to the acyltransferase activity, TGase 2 functions as binding and/or signaling protein. The enzyme is able to bind to fibronectin, a main component of the extracellular matrix (ECM), and integrins as well as to syndecan-4 on the cell surface. In this way, TGase 2 influences the RGD-independent adhesion, migration, signaling and differentiation of cells [5]. Depending on various regulatory factors, the localization of TGase 2 in the cell, and the associated biochemical environment, the enzyme exhibits different conformations that ultimately determine its function. In this context, Ca^{2+} ions and GTP/GDP act as inverse regulators of the acyltransferase activity of TGase 2. When Ca^{2+} is bound, TGase 2 adopts an open conformation in which the acyltransferase domain is accessible to the substrates. When GTP/GDP is bound, however, a closed conformation dominates in which the β-barrels interact non-covalently with the catalytic core and thus block the acyltransferase domain [6, 7]. Within cells, TGase 2 has been mainly detected in the cytoplasm but can also occur in the nucleus and the mitochondria and on the cell membrane as well as in the extracellular space, and it possesses the ability to translocate in between these compartments [8].

TGase 2 is expressed by many cell types, including endothelial cells, macrophages, and fibroblasts, and it regulates multiple processes during the tissue response following injury or implantation of a foreign material [9, 10]. In the early inflammatory reaction phase, TGase 2 promotes the extravasation and migration of neutrophils and monocytes to the injured tissue site, particularly in the presence of fibronectin [11]. Then, monocytes differentiate into macrophages and, simultaneously, the synthesis and activity of TGase 2 is enhanced. In macrophages, TGase 2 is required for phagocytosis [12]. During wound healing and tissue remodeling, TGase 2 plays an important role at later stages of the tissue response. The enzymatic and structural functions of TGase 2 promote the stabilization of the ECM and cell adhesion, thereby supporting wound healing [13]. Additionally, it was shown that TGase 2 immobilizes the vascular endothelial growth factor (VEGF) in the ECM and thus promotes angiogenesis [14]. *In vivo*

experiments with TGase 2-deficient mice confirmed the importance of the enzyme during tissue repair, as these mice showed delayed and impaired wound healing [15]. TGase 2 is furthermore involved in progressive scarring and fibrosis by the excessive cross-linking of matrix proteins, which was demonstrated for several fibrotic diseases in the lung, liver, kidney, heart and vasculature [13].

It is yet still unknown whether TGase 2 actions also contribute to the reaction of cells and tissue toward gelatin-based biomaterials. To investigate this, we selected two hydrogels formed from gelatin and L-lysine diisocyanate in different molar ratios,[16] which are well characterized with regard to their *in vitro* and *in vivo* behavior. In previous studies, these materials showed a good histocompatibility and suitable cellular adhesion and infiltration behavior as well as partly altered protein expression of cells.[17] Moreover, *in vivo,* they induced local mechanisms of tissue remodeling leading to a complete restoration of original tissue. They were completely degradable within 3 months and caused neither capsule formation nor fibrosis [17, 18].

In this study, this well characterized model of biomaterial implantation was used to investigate whether TGase 2 is present at the biomaterial-tissue interface and might serve as an informative biomarker for the visualization of tissue response toward biomaterials. For this purpose, the expression and activity of TGase 2 in response to gelatin-based hydrogels both *in vitro* and *in vivo* was studied. TGase 2 activity was probed by the incorporation of fluorescently labeled cadaverine derivatives into tissue sections. These cadaverines were recently described as acyl acceptor substrates of TGase 2 for application in a fluorescence anisotropy-based assay, which detects the TGase 2 acyltransferase activity and allows for high-throughput screening of TGase 2 inhibitors as well as measuring of TGase 2 activity in cell lysates [19, 20]. As these cadaverines might also act as amine substrates for other TGases, such as TGases 1 or 3 (unpublished data), selectivity of their incorporation was confirmed by application of a selective TGase 2 inhibitor.[20, 21] In addition, the Rhodamine B-labeled cadaverine derivative was tested for functional optical imaging of TGase 2 activity at implantation sites.

.

Materials and Methods

Hydrogel synthesis and eluate preparation

The two gelatin-based hydrogels G10_LNCO3 and G10_LNCO8 were synthesized and sterilized as described previously.[16] Briefly, a 10 wt.-% aqueous gelatin solution (from porcine skin, 200 bloom, type A, low endotoxin content, GELITA) was treated in the presence of 1 wt.-% poly(ethylene glycol)-*block*-poly(propylene glycol)-*block*-poly(ethylene glycol) (Pluronic® F-108, Sigma-Aldrich) with different amounts of lysine diisocyanate ethyl ester [LDI, 3-fold (G10_LNCO3) or 8-fold (G10_LNCO8) molar ratio NCO/NH_2 groups of gelatin]. Hydrogels were sterilized by ethylene oxide sterilization. For cell culture experiments, a hydrogel film with a diameter of 10 cm was incubated in 20 mL of phosphate buffered saline (PBS, pH 7.4, 274 mM NaCl, 5.4 mM KCl, 3 mM KH_2PO_4, 14.6 mM Na_2HPO_4, 0.5 mM $MgCl_2 \cdot 6 H_2O$, 1 mM $CaCl_2 \cdot 2 H_2O$) overnight. The supernatant was removed and 6-well or 96-well sized hydrogel pieces were cut out. Additionally, hydrolytic and enzymatic hydrogel eluates were prepared to evaluate the influence of hydrogel degradation products on the cells [17]. The supernatants after 72 h of incubation of a hydrogel film with a diameter of 10 cm in 35 mL of suitable, serum-free medium containing 1 U/mL penicillin/streptomycin (P/S, Biochrom) were defined as hydrolytic eluates. In contrast, enzymatic eluates were received by the addition of 5×10^{-6} wt.-% model protease trypsin (250 USP U/mg) and 2×10^{-6} wt.-% EDTA (Biochrom) to elution medium. Eluates were supplemented with 2 vol.-% fetal calf serum (FCS, Biochrom). For implantations, 10 hydrogel pieces with a size of 3 × 10 mm were incubated in 20 mL PBS for 1 h [17].

Cell culture and protein expression *in vitro*

Cell culture and sample preparation for protein analysis were performed as previously described[17]. Briefly, human aortic endothelial cells (HAEC, Pelobiotech) were cultured in endothelial cell growth medium enhanced containing 0.5 ng/mL soluble vascular endothelial growth factor (Pelobiotech). Human acute monocytic leukemia cell line THP-1 and human acute myeloid leukemia cell line HL-60 (both from ECACC) were cultured in RPMI 1640 medium (Biochrom) supplemented with 10 vol-% FCS and 1 U/mL P/S. THP-1 and HL-60 cells were differentiated to macrophage-like cells (THP-1 Mϕ and HL-60 Mϕ) by treatment with 64 nM 12-*O*-tetradecanoylphorbol-13-acetate (TPA, Sigma-Aldrich) for

72 h. HL-60 cells were differentiated to granulocyte-like cells (HL-60 Gϕ) by treatment with 1.3 vol-% dimethyl sulfoxide (DMSO, Fisher BioReagents) for 6 days.

In order to investigate cellular TGase 2 synthesis and secretion in response to direct contact to the hydrogels, cells were cultured directly on G10_LNCO3 and G10_LNCO8 in 6-well plates (1×10^6 cells/well in 5 mL medium) for 48 h. Additionally, to determine the influence of hydrolytic or enzymatic degradation products of the hydrogels, cells were seeded in 6-well plates (5×10^5 cells/well HAEC, 3×10^6 cells/well THP-1 Mϕ and HL-60 Mϕ, 1×10^7 cells/well HL-60 Gϕ) and incubated with 5 mL eluate/well for 48 h. Cultivation with cell culture medium served as control. Cells were harvested by incubation with 2 mM EDTA in PBS for 30 min, centrifugation at 300*g* for 5 min, and collection of cell pellet in 100 µL RIPA lysis buffer (150 mM NaCl, 50 mM Tris, pH 8.0, 1 % NP40, 0.5 wt.-% SDS, 7 µg/mL leupeptin, 1 mM PMSF, 1 mM Na_3VO_4, 1 mM DTT, 7 mM NaF). 2 mL of cell culture supernatant was prepared for protein analysis by centrifugation at 300 × g for 5 min to remove the remaining cells out of the supernatant, which was transferred to a new tube and centrifuged again at 3000*g* for 15 min. Afterwards, 1800 µL of the supernatant were removed. Lysis of cells, SDS-PAGE, and Western Blotting were performed as described previously.[22] Blots were incubated with primary antibodies against TGase 2 (ab2386, Abcam, 1:500, mouse) and β-actin (A5316, Sigma-Aldrich, 1:1000, mouse) and secondary antibody antimouse IgG POD (A9044, Sigma-Aldrich, 1:2000/1:10000, polyclonal rabbit). Blots were evaluated by densitometric and statistical analysis as described previously [17].

Distribution of TGase 2 in the cells was visualized by immunocytochemistry. HAEC were seeded directly on the hydrogels in 96-well plates (33×10^4 cells/well in 200 µL of medium) for 48 h. Again, cultivation with cell culture medium served as control. Cells were fixed for 30 min with 4 wt.-% PFA and 2.5 wt.-% sucrose in water and permeabilized for 10 min in methanol at -20 °C. Unspecific binding was blocked for 1 h with 10 vol.-% FCS in Tris-buffered saline (TBS, 10 mM Tris pH 7.4, 150 mM NaCl), and cells were incubated with primary antibodies against TGase 2 (ab2386, Abcam, 1:50, mouse), actin (A5060, Sigma-Aldrich, 1:100, rabbit), and isotype control (normal mouse IgG, sc2025, Santa Cruz Biotechnology, 1:100) overnight. Subsequently, cells were incubated with fluorescently labeled secondary antibodies against mouse (IgG-Alexa Fluor 488, A11029, Thermo Scientific, 1:200, polyclonal goat) and rabbit (IgG-Alexa Fluor 647, A21245, Thermo Scientific, 1:200, polyclonal goat) for 1 h. Cell nuclei were stained for 20 min with 5 mg/mL HOECHST 33258 (Sigma-Aldrich) in TBS. Cells were imaged using confocal laser scanning microscopy (FV10_ASW, Olympus).

Animals, hydrogel implantation and protein expression *in vivo*

The performance of animal experiments was in accordance to the guidelines of the German Regulations of Animal Welfare, and the applied protocol was approved by local Ethical Committee for Animal Experiments (reference number 24-9168.11-4/2013-1). Immunocompetent and hairless female SKH1-Elite mice were purchased from Charles River. One swollen hydrogel piece was implanted subcutaneously at the lower dorsal area of a mouse as described previously [17, 18]. Briefly, mice were anesthetized using 10 vol.-% desfluran (Baxter). A small incision was made in the implantation area, a skin pocket was formed using a surgical scissors, and the hydrogel was inserted into the pocket. The wound was closed with spray dressing. Mice received analgesic Rimadyl (5 mg/kg) as single injection.

Hydrogels with surrounding tissue were explanted at selected time points after implantation (days 1, 7, 14, 21, 28, 35, 56, 84, and 112), and samples were bisected. One half was used for Western Blot analysis and collected in 300 µL RIPA lysis buffer. Samples were lysed for 9 min at 25 Hz in a tissue lyser (Qiagen). SDS-Page, Western Blotting, and subsequent densitometric and statistical analysis were performed as described above for the cell culture experiments. Different from above, GAPDH was used as reference protein for TGase 2 using a primary antibody against GAPDH (G8795, Sigma Aldrich, 1:5000, mouse). The other half of the sample was used for immunohistochemical staining of TGase 1, TGase 2, TGase 3, and FXIIIa, which was performed as described previously [17, 18]. Briefly, samples were fixed by treatment with 4 wt.-% PFA and 2.5 wt.-% sucrose in water for 24 h and 20 wt.-% sucrose in PBS for 3 days. Samples were embedded in 7.5 wt.-% gelatin/ 20 wt.-% sucrose in PBS, frozen, and cryosliced. Sections were pretreated in 10 mM citrate buffer (pH 6.0) and heated for 20 min before quenching of endogenous peroxidase for 10 min in 3 vol.-% hydrogen peroxide solution, and blocking of unspecific binding for 1 h in 10 vol.-% FCS in TBS was performed. Sections were incubated with primary antibodies against TGase 1 (ab103814, Abcam, 1:200, rabbit), TGase 2 (sc20621, Santa Cruz Biotechnology, 1:50, rabbit), TGase 3 (ab203229, Abcam, 1:200, rabbit), and FXIIIa (ab97636, Abcam, 1:200, rabbit), or isotype control (normal rabbit IgG, sc2027, Santa Cruz Biotechnology, 1:40) overnight. Subsequently, sections were incubated with biotinylated secondary antibody against rabbit (IgG-biotinylated, 111-065-003, Dianova, 1:200, goat) for 1 h, which was visualized by incubation with ExtrAvidin peroxidase (Sigma-Aldrich) for 30 min and an AEC substrate kit (BD Biosciences) for 2 – 10 min. Sections were counterstained with Mayer's hematoxylin and embedded in aqueous solution.

Sections were imaged using an AxioImager.A1 microscope and AxioVision software (Carl Zeiss). Quantification of the immunohistochemical stainings was performed using ImageJ (version 1.52i). The color threshold plugin was used, and RGB values were set for immunohistochemically positive stained areas before applying the Analyze Particles Plugin. This was repeated for 3 animals per hydrogel and time point.

TGase activity in tissue sections

Hydrogels with surrounding tissue were explanted at selected time points after implantation (days 15, 28, and 84), embedded in 7.5 wt.-% gelatin/ 20 wt.-% sucrose in PBS, frozen, and cryosliced. Sections were placed immediately in TGase activation buffer (MOPS pH 8.0, 3 mM $CaCl_2$, 50 µM EDTA, 5 mM DTT) and were treated with 10 µM of a selective TGase 2 inhibitor N^{α}-phenylacetyl-N^{ε}-acryloyl-lysine-4-(6-methylpyridine-2-yl)piperazide (**1**), N^{α}-phenylacetyl-N^{ε}-acryloyl-lysine-4-(6-fluoropyridine-2-yl)piperazide **(2)**, or activation buffer for 0.5 or 1 h at 37 °C (Figure 3A). Compounds **1** and **2** were synthesized and characterized as previously described. [20, 21] Sections were incubated with 0.1 mM Rhodamine-B-isonipecotyl-cadaverine (**R-I-Cad**, Figure 3A) or 5'-[(5-aminopentyl)thioureidyl]-fluorescein (**F-Cad**, Figure 3A) for 4 h at 37 °C in the presence or absence of inhibitors **1** and **2**. Synthesis of fluorescently labeled cadaverines was performed as previously described. [19] Sections were fixed for 3 × 5 min at -20 °C in methanol, blocked for 1 h in 10 vol.-% FCS in TBS, and incubated with primary antibody against TGase 1 (as103814, Abcam, 1:200, rabbit), TGase 2 (sc20261, Santa Cruz Biotechnology, 1:50, rabbit), TGase 3 (ab203229, Abcam, 1:200, rabbit), and FXIIIa (ab97636, Abcam, 1:200, rabbit) or isotype control (normal rabbit IgG, sc2027, Santa Cruz Biotechnology, 1:40) overnight. Subsequently, sections were incubated with secondary antibody against rabbit (IgG-Alexa Fluor 647, A21245, Thermo Scientific, 1:200, polyclonal goat or IgG-Alexa Fluor 488, A21206, Thermo Scientific, 1.200, polyclonal donkey) for 1 h. Cell nuclei were stained for 20 min with 5 mg/mL HOECHST 33258 (Sigma-Aldrich) in TBS. Sections were imaged using confocal laser scanning microscopy (FV1000_ASW, Olympus). Hydrogels shrank due to dehydration by methanol during the staining process.

Toxicity of F- and R-I-Cad

The toxicity of **F-Cad** and **R-I-Cad** toward MeWo and A375 melanoma cells, which represent models of substantially different TGase 2 expression (MeWo do not express TGase 2, and A375 express TGase 2 to a high extend) was tested by CellTiterBlue and LDH assay, respectively. Different assays were used due to overlapping absorbance/emission spectra of fluorescein and formazan (LDH assay) as well as Rhodamine B and Resorufin (CellTiter Blue assay). Cells were seeded in 96-well plates (40 000 A375/well or 50 000 MeWo/well in 200 µL of RPMI medium) and cultured overnight. Subsequently, the medium was removed, and cadaverine was added to a concentration of 10, 100, 250, 500, or 1000 µM in 200 µL of medium. Cell culture medium as vehicle served as a nontoxic control, and Triton X-100 at a concentration of 2 vol.-% served as a toxic control. After 2 and 22 h, 50 µL samples were taken for the LDH assay, or CellTiter Blue reagent was added to the cells. The LDH assay (Pierce LDH Cytotoxicity Assay Kit, 88953, Thermo Scientific) as well as CellTiter Blue assay (CellTiter-Blue® Cell Viability Assay, G8080, Promega) were performed according to the manufacturer's instructions. The statistical significance of data was evaluated by two-way ANOVA coupled with a *post hoc* Bonferroni correction analysis. P values below 0.05 were considered significant and are depicted as *.

In vivo fluorescence imaging of R-I-Cad distribution

In a pilot study, **R-I-Cad** was injected in non-implanted mice and mice bearing G10_LNCO3 or G10_LNCO8 14 and 15 days after implantation. For injection, **R-I-Cad** was resalted by dissolution in 0.1 M HCl and subsequent lyophilization of that solution. In order to determine the optimal dosage with no observed adverse effect level (NOAEL), 3 different doses (0.04 mg/kg = 0.56 mmol/kg, 0.4 mg/kg = 5.6 mmol/kg, and 4 mg/kg = 56 mmol/kg), dissolved in 100 µL of isotonic sodium chloride solution, were administered intravenously in two mice each. In a second experiment, 0.4 mg/kg R-I-cadaverine was administered in 3 different ways (intravenously, intraperitoneally, and subcutaneously) in 3 mice each. At selected time points after injection (3 min, 10 min, 1 h, 24 h), *in vivo* fluorescence imaging using the small animal optical imaging device *in vivo* Xtreme (Bruker) with Bruker Molecular Imaging software version 7.2 was performed. A 550 nm excitation filter and a 600 nm emission filter were used, and a reference image (440/500 nm) for nonspecific fluorescence as well as an X-ray image were acquired.

Results

Hydrogel contact affected the synthesis and secretion of TGase 2 by endothelial and immune cells *in vitro*

Synthesis and secretion of TGase 2 by different cell types was analyzed in vitro after direct exposure to the hydrogels or after cultivation in the presence of their eluates. Hydrogel eluates were produced by hydrolytic and enzymatic degradation of the materials and, therefore, contain either hydrolytic or hydrolytic and enzymatic degradation products of the hydrogels. We evaluated whether direct contact between cells and hydrogels is necessary to influence TGase 2 or whether degradation products could also induce any effect.

Human aortic endothelial cells (HAEC) synthesized high amounts of TGase 2, independent from contact to hydrogels or their eluates. Additionally, they showed a high secretion of TGase 2, which was different for both hydrogels (Figures 1A and S1). Visualization by immunohistochemistry revealed TGase 2 to be located in the cytoplasm and in vesicles at the cell membrane (Figure 1B). Human acute monocytic leukemia cells, differentiated to macrophages (THP-1 Mϕ), synthesized higher amounts of TGase 2 after contact to hydrogel eluates, while direct hydrogel contact did not influence TGase 2 synthesis. The cells secreted TGase 2 only to a small extent, which slightly increased after direct hydrogel contact (Figures 1A and S1). In contrast, human acute myeloid leukemia cells, differentiated to granulocytes (HL-60 Gϕ) or macrophages (HL-60 Mϕ), showed a significantly enhanced synthesis of TGase 2 after direct contact to the hydrogels, whereas contact to their hydrolytic or enzymatic degradation products did not cause a reaction. Both cell types did not secrete TGase 2 (Figures 1A and S1). bis hierher

Hydrogel implantation enhanced the synthesis of TGase 2 *in vivo*

Hydrogels G10_LNCO3 or G10_LNCO8 were implanted subcutaneously into immunocompetent nude SKH1-Elite mice. At selected time points after implantation (days 1, 7, 14, 21, 28, 35, 56, 84, and 112), the hydrogels with surrounding tissue were explanted and the samples were analyzed regarding TGase 2 expression via different methods. In both hydrogels, we found no significant changes in TGase 2 synthesis when compared to normal skin as control (Figures 1C and S2). This might be due to the high standard errors that occur in the densitometric analysis, which are caused by the inhomogeneous

distribution of TGase 2 in the tissue. At later time points, however, we observed a trend toward a higher TGase 2 synthesis for both hydrogels.

In contrast, the analysis by immunohistochemistry showed increasing TGase 2 synthesis in the edge region of both hydrogels, beginning from day 7 until day 21 for G10_LNCO3 and day 35 for G10_LNCO8 (Figure 2A and B). Notably, TGase 2 was primarily detected in regions with the highest cell infiltration into the hydrogels. At later stages, TGase 2 synthesis remained constant until hydrogel degradation was completed (day 42 for G10_LNCO3 and day 84 for G10_LNCO8). Subsequently, no enhanced TGase 2 synthesis was detected in the implantation area.

Hydrogel implantation in part enhanced the synthesis of TGase 1, 3 and FXIIIa *in vivo*

We also performed immunohistochemical analyses for the expression of TGase 1 and 3 and FXIIIa at selected time points following implantation (Figure 2A,B). TGase 1, also known as keratinocyte TGase, was not detected in the hydrogel implantation areas. In contrast, TGase 3, the epidermal TGase, was synthesized by the cells, which are in direct contact to the hydrogels beginning from day 7 after implantation. Synthesis of TGase 3 increased until day 21 for G10_LNCO3 and day 35 for G10_LNCO8 and decreased again until the degradation of the hydrogels was completed. Afterward, a low and diffuse distribution of TGase 3 was determined. The synthesis of the terminal factor of the blood coagulation cascade FXIIIa, which is expressed by dermal dendrocytes among others, increased until day 21 after implantation of G10_LNCO3 and day 35 for G10_LNCO8. Within the first week, FXIIIa was detected in close proximity to the implanted hydrogels and later further away from the hydrogel−tissue interface. Beginning from day 21 after implantation of G10_LNCO3 and day 35 for G10_LNCO8, the synthesis of FXIIIa decreased and remained low and diffuse following the complete degradation of the hydrogels.

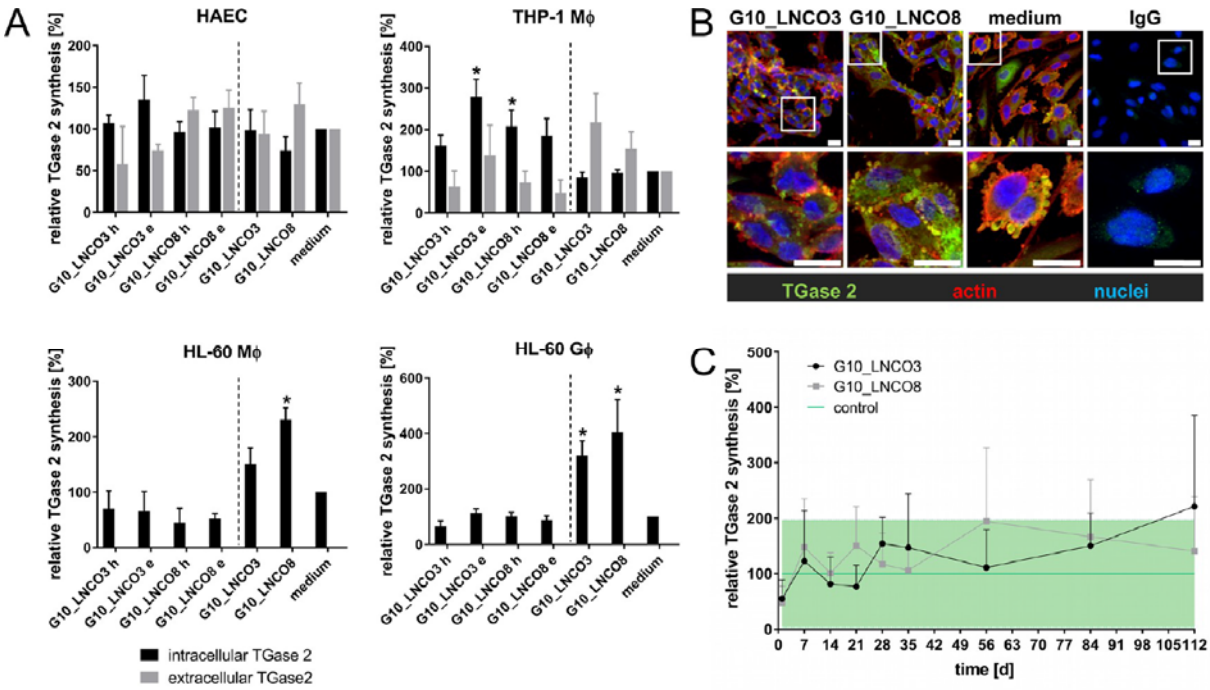

Figure 1: Synthesis and secretion of TGase 2 *in vitro* and synthesis of TGase 2 *in vivo.*

A: Synthesis and secretion of TGase 2 by HAEC, THP-1 Mϕ, HL-60 Mϕ, and HL-60 Gϕ after 48 h of direct contact to the hydrogels G10_LNCO3 and G10_LNCO8 or their hydrolytic (_h) or enzymatic (_e) eluates (separated by dotted line) were investigated by Western blotting. Cultivation with cell culture medium served as a control. Analysis of the blots was performed via densitometry, and data were related to β-actin as loading control and cultivation with cell culture medium (set to 100 %). n ≥ 3, mean ± SEM, *$p < 0.05$ vs. medium, ANOVA, Bonferroni *post hoc* test.

B: The intracellular distribution of TGase 2 in HAEC directly contacting the hydrogels or medium as a control was visualized via immunocytochemistry. IgG designates the staining with isotype control. TGase 2 is depicted in green, while actin is in red and cell nuclei are in blue. The scale bars indicate 20 µm.

C: TGase 2 synthesis in G10_LNCO3 and G10_LNCO8 implantation areas was investigated over a period of 112 days after implantation by Western blotting. Analysis of the blots was performed via densitometry, and data were related to GAPDH as loading control and control skin (set to 100 %). The green area reflects the range of TGase 2 synthesis in unwounded skin as a control. n ≥ 3, mean ± SEM, ANOVA, Bonferroni *post hoc* test.

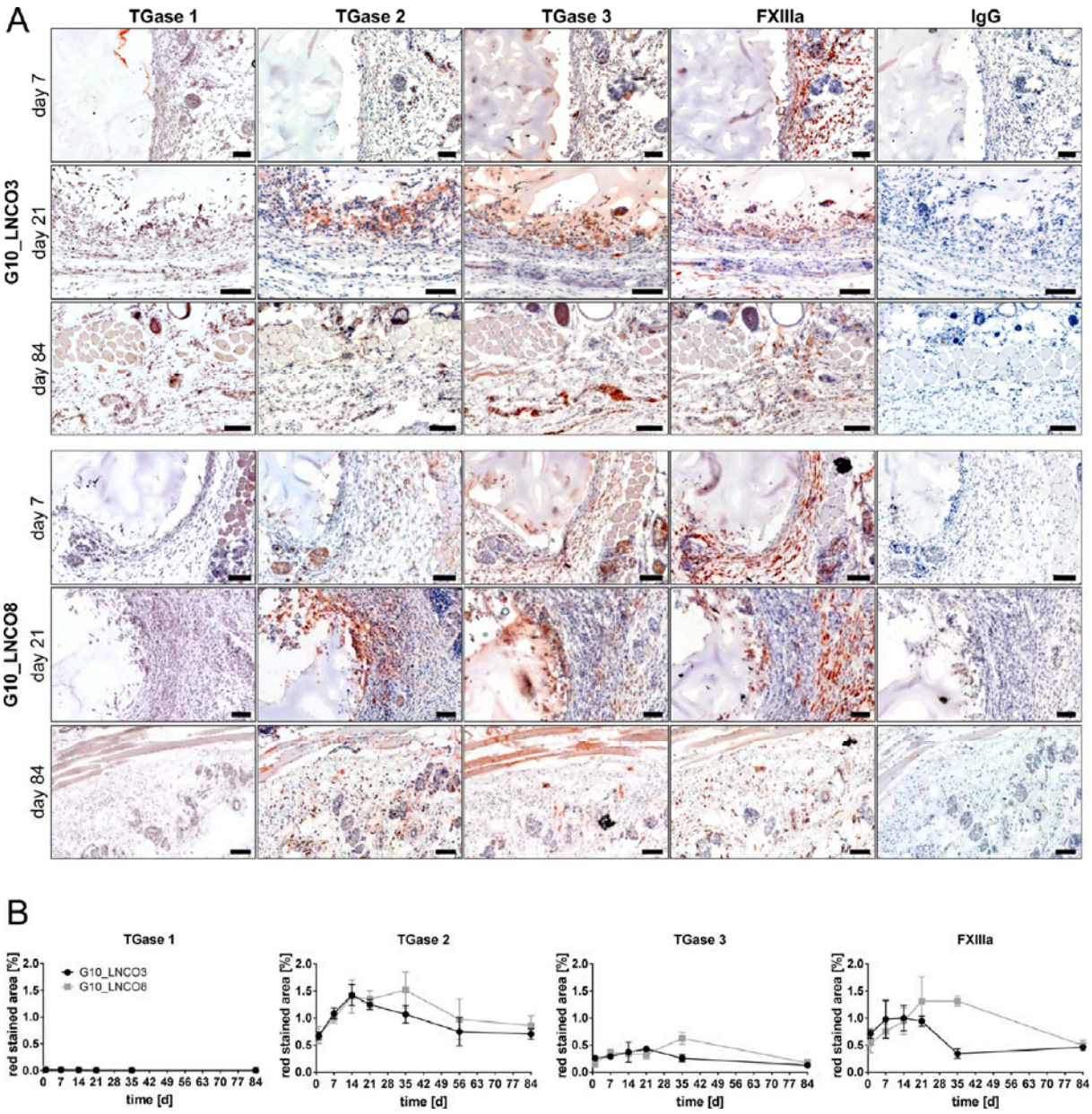

Figure 2. Synthesis of TGase 1, TGase 2, TGase 3, and FXIIIa in vivo.

(A) Synthesis of TGase 1, 2, and 3 and FXIIIa in G10_LNCO3 and G10_LNCO8 implantation areas was investigated at selected time points after implantation by immunohistochemistry. IgG designates the staining with isotype control. TGase is depicted in brown, while cytoplasm is in light pink and cell nuclei are in blue. The scale bars indicate 100 µm.

(B) Immunohistochemical staining of TGase 1, 2, and 3 and FXIIIa in G10_LNCO3 and G10_LNCO8 implantation areas was quantified using ImageJ. Graphs depict the red stained area over time.

TGase 2 was active as Acryltransferase around the implanted hydrogels

We next investigated the TGase activity around the implanted hydrogels at selected time points following implantation by incorporation of two fluorescently labeled TGase substrates, **R-I-Cad** and **F-Cad** into tissue sections (Figure 3A). Staining with TGase 2 antibodies revealed the colocalization of TGase 2 and incorporation of cadaverines (Figures 3B and S4). Without the addition of dithiothreitol (DTT) to the activation buffer, which inhibits the oxidation of SH residues to disulfide bridges, we found noincorporation of cadaverines (Figure S3A). Moreover, the addition of the selective TGase 2 inhibitor 1 (Figure 3A) considerably diminished the incorporation of cadaverines (Figures 3B and S4), suggesting that TGase 2 is the main TGase that is responsible for R-I-Cad incorporation, although other TGase isozymes also seem to mediate the transamidation reaction, however, to a minor extent.

In order to determine the extent of the transamidation reaction mediated by TGase 2 in comparison to TGase 1, TGase 3, and FXIIIa, the immunofluorescent detection of the mentioned TGases was compared to the incorporation of R-ICad. As exemplarily shown for the implantation area 15 days after implantation of G10_LNCO8, R-I-Cad incorporation mainly colocalized with TGase 2 and not with one of the other investigated TGases (Figure 4). Again, the addition of TGase 2 selective inhibitor 2 considerably inhibited incorporation of RI- Cad (Figure 4; further time points and G10_LNCO3 implantation areas as well as isotype controls are shown in Figures S5−S10). In this context, blocking experiments were performed by preincubation of the tissue section with the inhibitor for 1 h, followed by a coincubation with the cadaverine derivative for 4 h. Although compounds 1 and 2 were proven to be highly selective for TGase 2, they also act as irreversible inhibitors of the other TGases, when given a sufficient period of time for the reaction. Therefore, applying the above-mentioned procedure with an overall incubation period of 5 h could be improper to distinguish TGase 2 activity from other TGase activities. However, preincubation with TGase 2 inhibitor 2 for only 30 min followed by R-I-Cad inthe absence of inhibitor diminished the fluorescence signal in a similar dimension compared to the 5 h blocking approach (Figure S3B). This confirmed TGase 2 to be the main TGase active in the implantation areas during wound healing and remodeling phases.

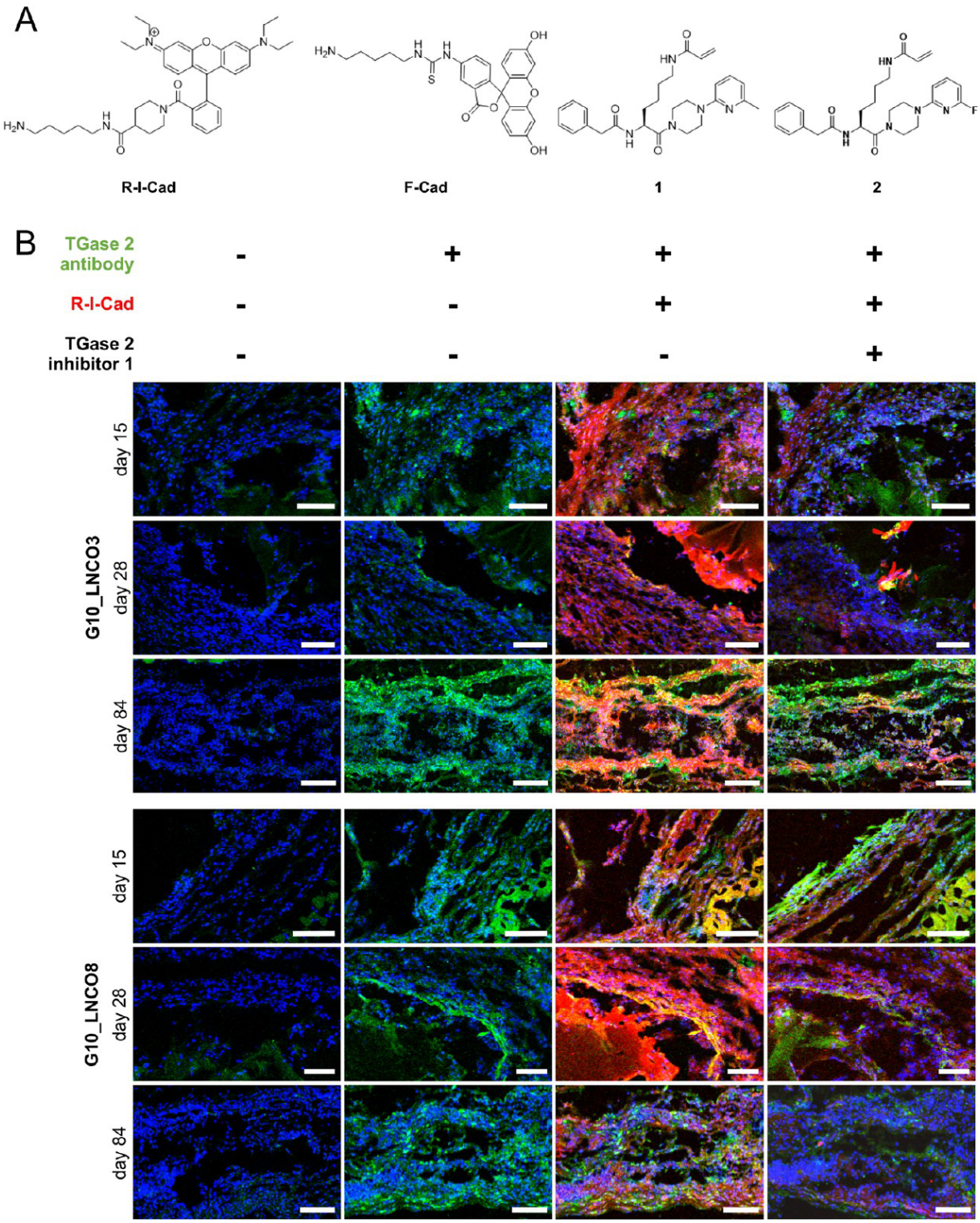

Figure 3: Cadaverine incorporation into tissue sections by active TGases

A: Structures of TGase substrates **R-I-Cad** and **F-Cad** and the selective TGase 2 inhibitor **1**[21] and **2**[20].

B: Incorporation of **R-I-Cad** by active TGases into tissue sections of G10_LNCO3 and G10_LNCO8 implantation areas was investigated at selected time points after implantation. Incorporation was inhibited by preincubation (1h) and coincubation (4h) with the selective TGase 2 inhibitor **1**. TGase 2 is depicted in green, while **R-I-Cad** is in red and cell nuclei are in blue. The scale bars indicate 100 µm.

F- and R-I-Cad were not toxic up to 500 µM

In order to test the fluorescently labeled cadaverines as potential imaging probes for active TGase 2, we next tested their cytotoxicity *in vitro* using two different toxicity tests with the MeWo and A375 cell lines (Figure 5). After a 2 h incubation, both **F-Cad** and **R-I-Cad** showed no toxicity up to a concentration of 1000 µM in either cell line compared to the vehicle treated controls and treatment with Triton X-100 as toxic control. After 22 h, **F-Cad** showed toxicity to MeWo at a concentration of 1000 µM, and **R-I-Cad** showed toxicity to MeWo and A375 at a concentration of 500 and 1000 µM, respectively. Treatment with 2 vol % Triton X-100 served as toxic control.

In vivo fluorescence imaging of R-I-Cad distribution showed no accumulation around the implanted hydrogels

In a pilot study, the suitability of **R-I-Cad** for noninvasive fluorescence imaging of TGase 2 activity was assessed by injection in nonimplanted mice and mice bearing G10_LNCO3 or G10_LNCO8 14 or 15 days following implantation. Dosages of 0.04, 0.4, and 4 mg/kg as well as intravenous, intraperitoneal, and subcutaneous routes of administration of **R-I-Cad** were tested. Using in vivo fluorescence imaging, we found no accumulation of **R-I-Cad** around the implanted hydrogels at different time points after the injection. For a detailed description of the results, please refer to the Supporting Information.

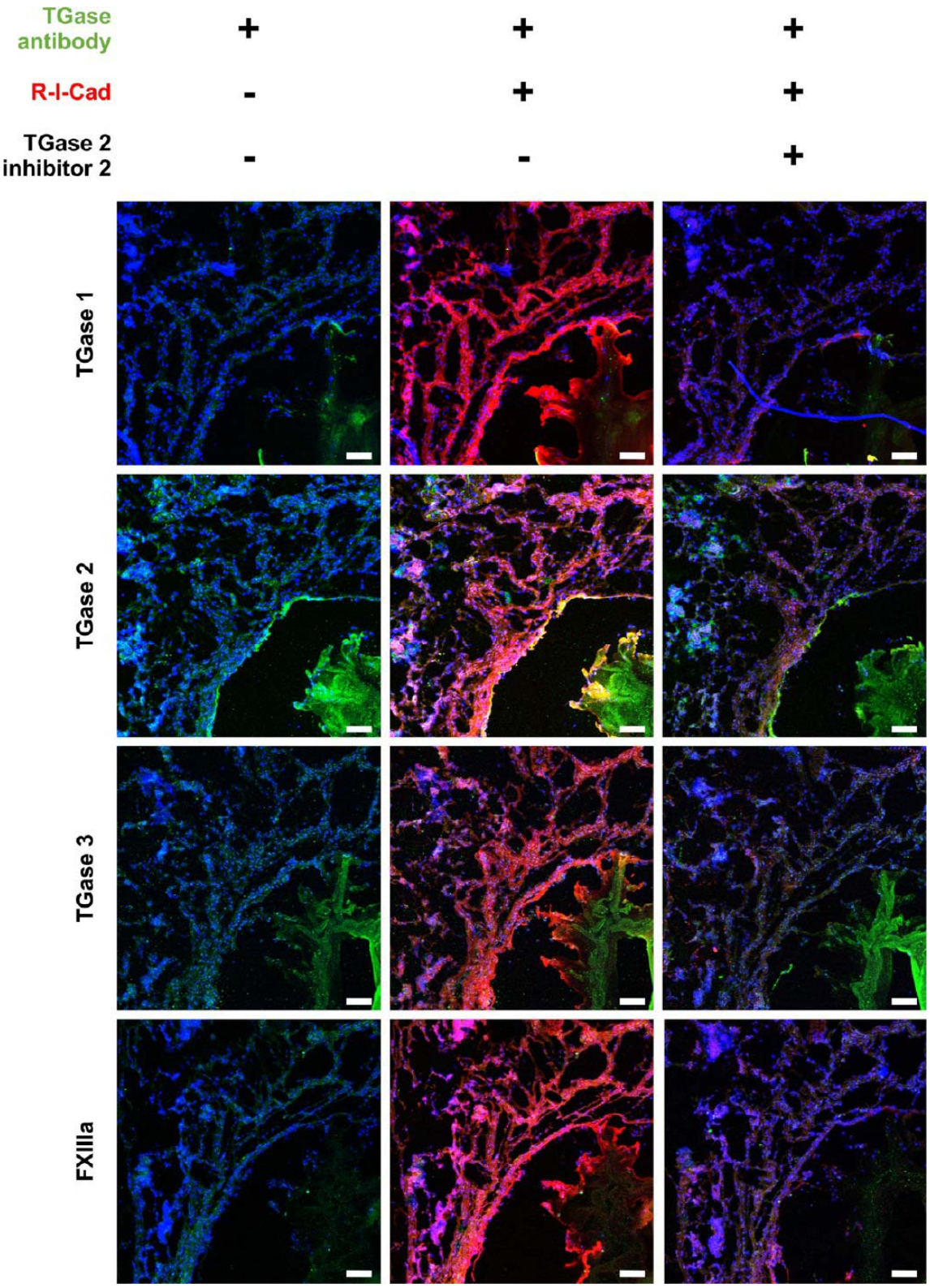

Figure 4: Colocalization of TGase 1, 2, and 3 and FXIIIa with cadaverine incorporation into tissue sections 15 days after implantation of G10_LNCO8. Immunofluorescence stainings of TGase 1, 2, and 3 and FXIIIa in the G10_LNCO8 implantation area 15 days after implantation and colocalization with the incorporation of **R-I-Cad**. Incorporation was inhibited by preincubation (1 h) and coincubation (4 h) with the selective TGase 2 inhibitor **2**. TGases are depicted in green, while **R-I-Cad** is in red and cell nuclei are in blue. The scale bars indicate 100 µm.

Discussion

The two gelatin-based hydrogels used in this study are well characterized regarding their *in vitro* and *in vivo* behavior. They differ in the cross-linking degree due to varying molar ratios between gelatin and lysine diisocyanate ethyl ester (LDI). The hydrogels induce a minor local inflammatory reaction, which supports tissue restoration. Moreover, they do not cause any sign of fibrosis and are completely degradable. [17, 18] Hence, they represent a model for a tissue response with a positive outcome. However, during the several phases of the tissue response induced by the hydrogels, TGase 2 might play an active role.

Starting at the cellular level, we first demonstrated the expression of TGase 2 by endothelial cells, macrophages, and granulocytes. This was partly influenced by contact to the hydrogels or their degradation products, however, without a clear correlation. In contrast, TGase 2 secretion differed remarkably between the different cells. Endothelial cells and THP-1-derived macrophages secreted TGase 2, whereas HL- 60-derived macrophages and granulocytes did not secrete TGase 2. This indicates two aspects of cellular differentiation. First, the cells could differ widely with regard to gene expression or secretion behavior, even if they are closely related or resemble a similar model (such as THP-1- and HL-60-derived macrophages).[17] Second, it suggests that secreted TGase 2 is involved in the cellular reaction towards gelatin-based hydrogels, as the secretion by all tested cell types was, at least partly, regulated by contact with them or their degradation products. Moreover, these cell-dependent patterns show that TGase 2 protein biosynthesis or secretion alone, without information on its molecular function, does not allow for conclusions about the possible consequences. One of the most important functions of the acyltransferase-inactive form of TGase 2 in macrophages is the direct interaction with a lactadherin-integrin complex on the cell surface, which is indispensable for phagocytosis of apoptotic cells [23]. Since phagocytosis by macrophages can also contribute to the degradation of hydrogels [24], TGase 2 might play an important role in the interaction of macrophages with hydrogels and their degradation products. In endothelial cells, TGase 2 was detected independently from the contact to the hydrogels primarily in the cytoplasm and in vesicles at the cell membrane. The localization of TGase 2 in the vesicles at the cell membrane could indicate the secretion process via endosome recycling as described by Zemskov and colleagues [25]. However, the observed vesicles could also be part of apoptotic processes [26]. Taken together, we show that secreted TGase 2 plays a role in

the interaction of the different cell types relevant during tissue response with gelatin-based hydrogels *in vitro*.

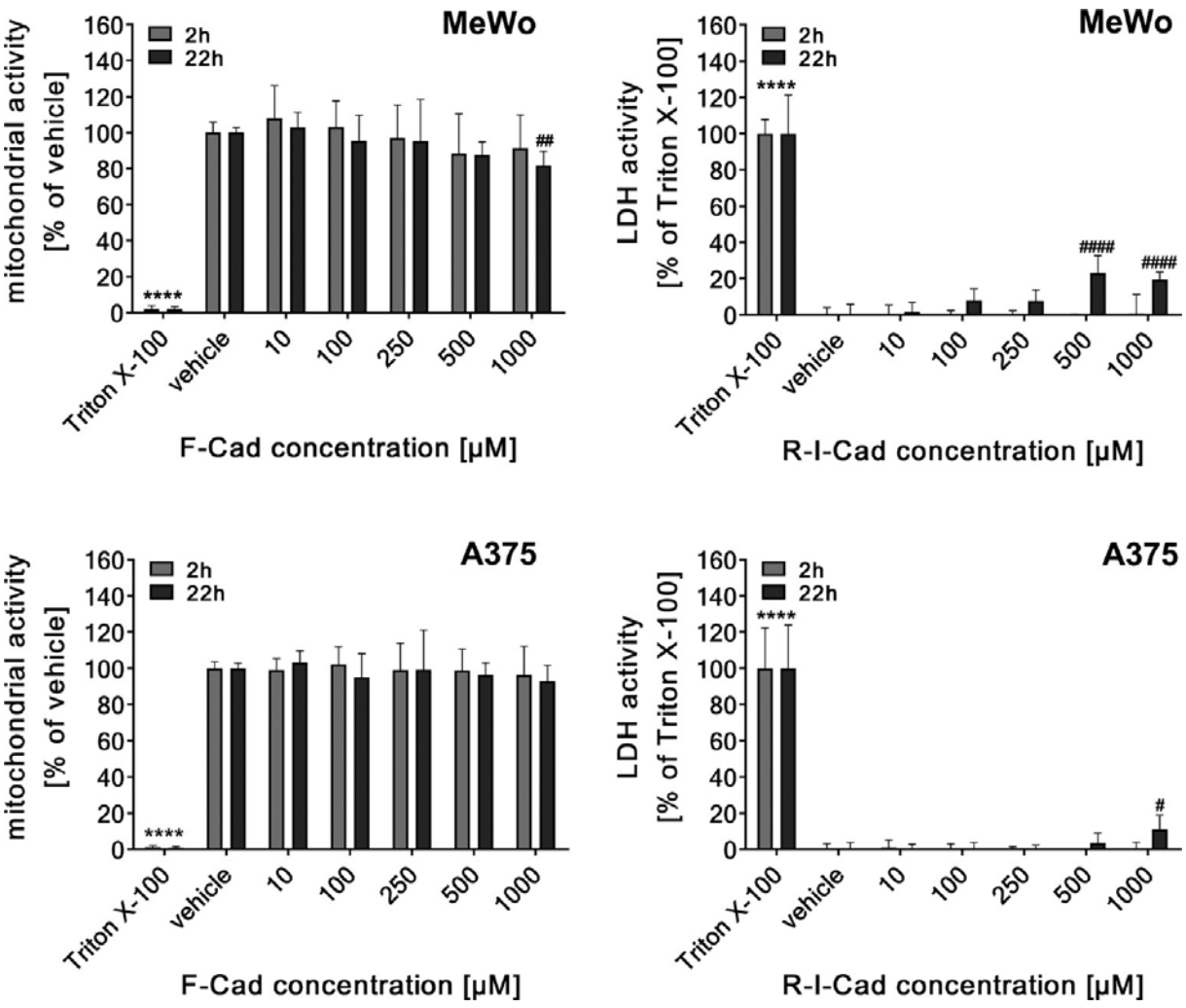

Figure 5. Cellular toxicity of F-Cad and R-I-Cad. The cellular toxicity of **F-Cad** was tested via the CellTiter Blue assay (left side), and the cellular toxicity of **R-I-Cad** was tested via the LDH assay (right side). n ≥ 4, mean ± SD, ****$p < 0.0001$ Triton X-100 vs all tested concentrations of cadaverine, ####$p < 0.0001$, ##$p < 0.01$, and #$p < 0.05$ cadaverine concentration vs vehicle, ANOVA, Bonferroni *post hoc* test.

In vivo, after the implantation of the hydrogels, no significant change of TGase 2 synthesis was detected by Western blot analysis. This, however, contradicted immunohistochemical stainings, which shows that Western blot analysis should not be used alone for assessing protein synthesis in inhomogeneous tissues. From day 7 to day 21 (G10_LNCO3) or day 35 (G10_LNCO8) after implantation, immunohistochemical results showed an increase in TGase 2 synthesis and a subsequent constant synthesis until complete degradation of the hydrogels. TGase 2 occurred primarily within the original dimensions of the implanted hydrogels. This indicates that detected TGase 2 was mainly synthesized

and secreted by immigrated macrophages (positive staining for CD68 as a pan-macrophage marker with similar time curve, performed in a previous study) [18, 27]. As already mentioned, the direct interaction of TGase 2 with a lactadherin-integrin complex on the cell surface of macrophages is crucial for their phagocytosis function, which can also contribute decisively to the degradation of the hydrogels [23]. Further, main functions of TGase 2 during wound healing include interactions with fibronectin secreted by fibroblasts for improved cell adhesion and migration as well as cross-linking of extracellular proteins for the formation and stabilization of ECM [13]. Studies by Park and colleagues showed that the activation of NF-κB by TGase 2 could lead to the induction of COX-2 synthesis in inflammatory regions, which correlates with the effects observed in our previous studies [17] and uncovers an additional link between wound healing and inflammation [28].

The experiments verified TGase 2 to be present at the biomaterial-tissue interface during tissue response, especially in places and phases of tissue remodeling. However, apart from TGase 2, eight other members of the TGase family are known in human: TGases 1, 3, 4, 5, 6, and 7, Factor XIIIa (FXIIIa), and erythrocyte membrane protein band 4.2 [29]. Among these, particularly TGase 1, whose expression is largely restricted to keratinocytes, TGase 3, the epidermal TGase, and FXIIIa, a blood coagulation factor expressed by dermal dendritic cells and macrophages among others, are of particular interest regarding skin wound healing and the hydrogel implantation scenario addressed in this study [29]. Therefore, we analyzed their expression profile in the implantation area. TGase 1 was not detected around the implanted hydrogels, which indicates that keratinocytes were not involved in the tissue response and, additionally, epidermal wound healing induced by the implantation process was already finalized at day 7 after implantation [30]. The synthesis of TGase 3 and FXIIIa was similar to that of TGase 2 in its temporal sequence, as it increased between day 7 and day 21/35, which was followed by a decrease to a low and diffuse expression level, which remained until hydrogel degradation was completed. In addition, TGase 3 colocalized with TGase 2 around the cells in direct contact with the implanted hydrogels. This finding contradicts the existing literature, where TGase 3 is described to be mainly expressed in outer, differentiating layers of stratified epithelia by keratinocytes [31, 32]. Compared to TGase 2 and TGase 3, the localization of FXIIIa synthesis was completely different and changed over time. In the beginning, FXIIIa was detected close to the implanted hydrogels and, after one week, it was localized further away from the hydrogel-tissue interface. Expressed mainly by dermal dendritic cells, FXIIIa fulfills an important role during wound healing by stimulating fibroblast proliferation and regulating

their collagen synthesis [33]. Together, this shows that not only TGase 2 but also other TGases, including TGase 3 or FXIIIa, are involved in the tissue response toward gelatin-based hydrogels.

As mentioned above, TGase 2 represents a multifunctional protein. Therefore, the information on its synthesis and secretion is not sufficient for defining its function during tissue response. In order to address this problem, we investigated the ability of TGase 2 surrounding the implanted hydrogels to act as acyltransferase by detection of the incorporation of two fluorescently labeled polyamines, **R-I-Cad** and **F-Cad**, into proteins of tissue sections. Polyamine derivatives labeled with reporter groups, such as biotin or fluorophores are established substrates for assessing TGase activity in living cells or tissues [34, 35]. For this assay, sections were incubated in a buffer (pH 8.0) containing $CaCl_2$ and DTT, which leads to activation of almost all of the present TGases by enhancing the Ca^{2+} content and inhibiting the oxidation of SH residues to disulfide bridges [36, 37]. An additional staining with antibodies against TGase 1, 2, and 3 and FXIIIa revealed colocalization of mainly TGase 2 and the incorporated cadaverine derivatives. In order to rule out that TGase 3 and FXIIIa, which were also surrounding the implanted hydrogels, caused the incorporation of the cadaverine derivatives, irreversible inhibitor selective for TGase 2 was applied. Pretreatment of the tissue sections with compound **1** or **2** almost completely attenuated incorporation of both amines. This indicates that TGase 2 can be activated as acyltransferase and confirms that it is the main TGase, which surrounds both implanted hydrogels. Moreover, this experiment showed that fluorescently labeled cadaverines are effective and easily detectable substrates of TGase 2. In this context, it should be noted that the applied conditions, especially the high concentration of the reducing agent DTT, are rather artificial and that the observed acyltransferase activity does not necessarily correspond to the activity of TGase 2 at the implantation site in living mice. Despite high Ca^{2+} and low GTP concentrations, extracellular TGase 2 is known to be mainly acyltransferase-inactive, since among other mechanisms, a nitric oxide-dependent modification of cysteine residues and a reversible intramolecular disulfide bridge between Cys370 and Cys371 can be formed, influencing its activity [38-40]. However, mechanical or inflammatory stimuli, which might be associated with a foreign biomaterial, can trigger the reduction of the disulfide bridge via thioredoxin and activate the acyltransferase function of TGase 2 [41]. To measure the potential *in situ* activity of TGase 2 around the implanted hydrogels, it was envisaged to use the fluorescently labeled cadaverine derivatives as probes for optical imaging in living mice.

In this respect, both cadaverine derivatives were tested for their cytotoxic effects. Within 2 h, neither **R-I-** nor **F-Cad** were toxic to two melanoma cell lines up to a concentration of 1000 µM, which was in concordance with the literature data for **FCad**.[42] As excitation and emission wavelengths of fluorescein are too short, it is not a suitable fluorophore for in vivo application. Hence, solely **R-I-Cad** was evaluated regarding the optimal dosage and application method in a pilot animal study. Nonimplanted mice and mice bearing one of the gelatin-based hydrogels were compared at time points with high TGase 2 synthesis and activity (14 or 15 days after implantation). No enrichment of **R-I-Cad** around the implanted hydrogels has been observed in any case. **R-I-Cad** remained at the injection site and was degraded and/or eliminated over time.

Conclusions

In this study, we demonstrated the time-dependent and cellspecific changes in TGase 2 expression, secretion, and activation upon implantation of gelatin-based hydrogels. On the basis of these results, TGase 2 can be considered as a potential informative biomarker for tissue response toward biomaterials. However, the tested conditions solely provide information on TGase 2 during positive tissue response. Therefore, to clearly define TGase 2 as a biomarker with predictive, diagnostic, discriminating, or prognostic value, future work should address the extent and duration of TGase 2 expression and activation in a model of negative tissue response to biomaterial implantation aiming to correlate TGase 2 to positive and negative outcomes. This will also allow the estimation of sufficient sensitivity and specificity to minimize both false negative and false positive results. Consequently, the development of suitable radiotracers, e.g., based on selective TGase 2 inhibitors, for positron or single photon emission tomography targeting TGase 2 can be envisaged. These will enable a quantitative functional characterization of the TGase 2 activity *in vivo*.

Acknowledgments

The excellent technical assistance of Aline Morgenegg, Mareike Barth, Catharina Knöfel and Sebastian Meister (HZDR) as well as the fabrication of hydrogels by Tim P. Gebauer and Peter Viszokai (Teltow) are greatly acknowledged. The authors thank Dr. Odette Leiter for proofreading the manuscript.The authors thank the Helmholtz Association for funding this work through programme-oriented funding and the Helmholtz Cross-Programme Initiative “Technology and Medicine – Adaptive Systems”. S.H. and J.P. are thankful to the Deutsche Forschungsgemeinschaft (DFG, German Research Foundation) for supporting this work in part within the Collaborative Research Center Transregio 67 “Functional Biomaterials for Controlling Healing Processes in Bone und Skin - From Material Science to Clinical Application“ (CRC/TRR 67/3; project number 59307082).

References

1. Pietsch, M.; Wodtke, R.; Pietzsch, J.; Löser, R., Tissue transglutaminase: an emerging target for therapy and imaging. *Bioorganic & medicinal chemistry letters* **2013,** 23, (24), 6528-43.
2. Wang, Z.; Griffin, M., TG2, a novel extracellular protein with multiple functions. *Amino acids* **2012,** 42, (2-3), 939-49.
3. Belkin, A. M., Extracellular TG2: emerging functions and regulation. *The FEBS journal* **2011,** 278, (24), 4704-16.
4. Fesüs, L.; Piacentini, M., Transglutaminase 2: an enigmatic enzyme with diverse functions. *Trends in biochemical sciences* **2002,** 27, (10), 534-9.
5. Telci, D.; Wang, Z.; Li, X.; Verderio, E. A.; Humphries, M. J.; Baccarini, M.; Basaga, H.; Griffin, M., Fibronectin-tissue transglutaminase matrix rescues RGD-impaired cell adhesion through syndecan-4 and beta1 integrin co-signaling. *The Journal of biological chemistry* **2008,** 283, (30), 20937-47.
6. Pinkas, D. M.; Strop, P.; Brunger, A. T.; Khosla, C., Transglutaminase 2 undergoes a large conformational change upon activation. *PLoS biology* **2007,** 5, (12), e327.
7. Liu, S.; Cerione, R. A.; Clardy, J., Structural basis for the guanine nucleotide-binding activity of tissue transglutaminase and its regulation of transamidation activity. *Proceedings of the National Academy of Sciences of the United States of America* **2002,** 99, (5), 2743-7.
8. Park, D.; Choi, S. S.; Ha, K. S., Transglutaminase 2: a multi-functional protein in multiple subcellular compartments. *Amino acids* **2010,** 39, (3), 619-31.
9. Thomazy, V.; Fesüs, L., Differential expression of tissue transglutaminase in human cells. An immunohistochemical study. *Cell and tissue research* **1989,** 255, (1), 215-24.
10. Telci, D.; Griffin, M., Tissue transglutaminase (TG2)--a wound response enzyme. *Frontiers in bioscience : a journal and virtual library* **2006,** 11, 867-82.
11. Akimov, S. S.; Belkin, A. M., Cell surface tissue transglutaminase is involved in adhesion and migration of monocytic cells on fibronectin. *Blood* **2001,** 98, (5), 1567-76.
12. Seiving, B.; Ohlsson, K.; Linder, C.; Stenberg, P., Transglutaminase differentiation during maturation of human blood monocytes to macrophages. *European journal of haematology* **1991,** 46, (5), 263-71.
13. Verderio, E. A.; Johnson, T.; Griffin, M., Tissue transglutaminase in normal and abnormal wound healing: review article. *Amino acids* **2004,** 26, (4), 387-404.
14. Wang, Z.; Perez, M.; Caja, S.; Melino, G.; Johnson, T. S.; Lindfors, K.; Griffin, M., A novel extracellular role for tissue transglutaminase in matrix-bound VEGF-mediated angiogenesis. *Cell death & disease* **2013,** 4, e808.
15. Mearns, B.; Nanda, N.; Michalicek, J.; Iismaa, S.; Graham, R., Impaired wound healing and altered fibroblast cytoskeletal dynamics in Gh knockout mice. *Minerva Biotechnologica* **2002,** 14, (2), 1.
16. Pierce, B. F.; Pittermann, E.; Ma, N.; Gebauer, T.; Neffe, A. T.; Hölscher, M.; Jung, F.; Lendlein, A., Viability of human mesenchymal stem cells seeded on crosslinked entropy-elastic gelatin-based hydrogels. *Macromolecular bioscience* **2012,** 12, (3), 312-21.
17. Ullm, S.; Krüger, A.; Tondera, C.; Gebauer, T. P.; Neffe, A. T.; Lendlein, A.; Jung, F.; Pietzsch, J., Biocompatibility and inflammatory response in vitro and in vivo to gelatin-based biomaterials with tailorable elastic properties. *Biomaterials* **2014,** 35, (37), 9755-9766.
18. Tondera, C.; Hauser, S.; Krüger-Genge, A.; Jung, F.; Neffe, A. T.; Lendlein, A.; Klopfleisch, R.; Steinbach, J.; Neuber, C.; Pietzsch, J., Gelatin-based Hydrogel Degradation and Tissue Interaction in vivo: Insights from Multimodal Preclinical Imaging in Immunocompetent Nude Mice. *Theranostics* **2016,** 6, (12), 2114-2128.
19. Hauser, C.; Wodtke, R.; Löser, R.; Pietsch, M., A fluorescence anisotropy-based assay for determining the activity of tissue transglutaminase. *Amino acids* **2017,** 49, (3), 567-583.
20. Wodtke, R.; Hauser, C.; Ruiz-Gomez, G.; Jäckel, E.; Bauer, D.; Lohse, M.; Wong, A.; Pufe, J.; Ludwig, F. A.; Fischer, S.; Hauser, S.; Greif, D.; Pisabarro, M. T.; Pietzsch, J.; Pietsch, M.; Löser, R., N(epsilon)-Acryloyllysine Piperazides as Irreversible Inhibitors of Transglutaminase 2: Synthesis, Structure-Activity Relationships, and Pharmacokinetic Profiling. *J Med Chem* **2018,** 61, (10), 4528-4560.
21. Wityak, J.; Prime, M. E.; Brookfield, F. A.; Courtney, S. M.; Erfan, S.; Johnsen, S.; Johnson, P. D.; Li, M.; Marston, R. W.; Reed, L., SAR development of lysine-based irreversible inhibitors of transglutaminase 2 for Huntington's disease. *ACS medicinal chemistry letters* **2012,** 3, (12), 1024-1028.
22. Wolf, S.; Haase-Kohn, C.; Lenk, J.; Hoppmann, S.; Bergmann, R.; Steinbach, J.; Pietzsch, J., Expression, purification and fluorine-18 radiolabeling of recombinant S100A4: a potential probe for molecular imaging of receptor for advanced glycation endproducts in vivo? *Amino acids* **2011,** 41, (4), 809-20.

23. Toth, B.; Garabuczi, E.; Sarang, Z.; Vereb, G.; Vamosi, G.; Aeschlimann, D.; Blasko, B.; Becsi, B.; Erdodi, F.; Lacy-Hulbert, A.; Zhang, A.; Falasca, L.; Birge, R. B.; Balajthy, Z.; Melino, G.; Fesüs, L.; Szondy, Z., Transglutaminase 2 is needed for the formation of an efficient phagocyte portal in macrophages engulfing apoptotic cells. *Journal of immunology* **2009,** 182, (4), 2084-92.
24. Sheikh, Z.; Brooks, P. J.; Barzilay, O.; Fine, N.; Glogauer, M., Macrophages, Foreign Body Giant Cells and Their Response to Implantable Biomaterials. *Materials* **2015,** 8, (9), 5269.
25. Zemskov, E. A.; Mikhailenko, I.; Hsia, R. C.; Zaritskaya, L.; Belkin, A. M., Unconventional secretion of tissue transglutaminase involves phospholipid-dependent delivery into recycling endosomes. *PloS one* **2011,** 6, (4), e19414.
26. Coleman, M. L.; Sahai, E. A.; Yeo, M.; Bosch, M.; Dewar, A.; Olson, M. F., Membrane blebbing during apoptosis results from caspase-mediated activation of ROCK I. *Nature cell biology* **2001,** 3, (4), 339-45.
27. Haroon, Z. A.; Hettasch, J. M.; Lai, T. S.; Dewhirst, M. W.; Greenberg, C. S., Tissue transglutaminase is expressed, active, and directly involved in rat dermal wound healing and angiogenesis. *FASEB journal : official publication of the Federation of American Societies for Experimental Biology* **1999,** 13, (13), 1787-95.
28. Park, M. K.; Cho, S. A.; Lee, H. J.; Lee, E. J.; Kang, J. H.; Kim, Y. L.; Kim, H. J.; Oh, S. H.; Choi, C.; Lee, H.; Kim, S. Y., Suppression of Transglutaminase-2 is Involved in Anti-Inflammatory Actions of Glucosamine in 12-O-Tetradecanoylphorbol-13-Acetate-Induced Skin Inflammation. *Biomolecules & therapeutics* **2012,** 20, (4), 380-5.
29. Eckert, R. L.; Kaartinen, M. T.; Nurminskaya, M.; Belkin, A. M.; Colak, G.; Johnson, G. V.; Mehta, K., Transglutaminase regulation of cell function. *Physiological reviews* **2014,** 94, (2), 383-417.
30. Inada, R.; Matsuki, M.; Yamada, K.; Morishima, Y.; Shen, S. C.; Kuramoto, N.; Yasuno, H.; Takahashi, K.; Miyachi, Y.; Yamanishi, K., Facilitated wound healing by activation of the Transglutaminase 1 gene. *Am J Pathol* **2000,** 157, (6), 1875-82.
31. Hitomi, K.; Horio, Y.; Ikura, K.; Yamanishi, K.; Maki, M., Analysis of epidermal-type transglutaminase (TGase 3) expression in mouse tissues and cell lines. *Int J Biochem Cell Biol* **2001,** 33, (5), 491-8.
32. Hitomi, K.; Presland, R. B.; Nakayama, T.; Fleckman, P.; Dale, B. A.; Maki, M., Analysis of epidermal-type transglutaminase (transglutaminase 3) in human stratified epithelia and cultured keratinocytes using monoclonal antibodies. *J Dermatol Sci* **2003,** 32, (2), 95-103.
33. Quatresooz, P.; Paquet, P.; Hermanns-Le, T.; Pierard, G. E., Molecular mapping of Factor XIIIa-enriched dendrocytes in the skin. *Int J Mol Med* **2008,** 22, (4), 403-9.
34. Lajemi, M.; Demignot, S.; Borge, L.; Thenet-Gauci, S.; Adolphe, M., The use of Fluoresceincadaverine for detecting amine acceptor protein substrates accessible to active transglutaminase in living cells. *The Histochemical journal* **1997,** 29, (8), 593-606.
35. Jeon, J. H.; Kim, C. W.; Shin, D. M.; Kim, K.; Cho, S. Y.; Kwon, J. C.; Choi, K. H.; Kang, H. S.; Kim, I. G., Differential incorporation of biotinylated polyamines by transglutaminase 2. *FEBS letters* **2003,** 534, (1-3), 180-4.
36. van der Wildt, B.; Wilhelmus, M. M.; Bijkerk, J.; Haveman, L. Y.; Kooijman, E. J.; Schuit, R. C.; Bol, J. G.; Jongenelen, C. A.; Lammertsma, A. A.; Drukarch, B.; Windhorst, A. D., Development of carbon-11 labeled acryl amides for selective PET imaging of active tissue transglutaminase. *Nuclear medicine and biology* **2016,** 43, (4), 232-42.
37. van der Wildt, B.; Wilhelmus, M. M.; Kooijman, E. J.; Jongenelen, C. A.; Schuit, R. C.; Büchold, C.; Pasternack, R.; Lammertsma, A. A.; Drukarch, B.; Windhorst, A. D., Development of fluorine-18 labeled peptidic PET tracers for imaging active tissue transglutaminase. *Nuclear medicine and biology* **2017,** 44, 90-104.
38. Siegel, M.; Strnad, P.; Watts, R. E.; Choi, K.; Jabri, B.; Omary, M. B.; Khosla, C., Extracellular transglutaminase 2 is catalytically inactive, but is transiently activated upon tissue injury. *PloS one* **2008,** 3, (3), e1861.
39. Stamnaes, J.; Pinkas, D. M.; Fleckenstein, B.; Khosla, C.; Sollid, L. M., Redox regulation of transglutaminase 2 activity. *The Journal of biological chemistry* **2010,** 285, (33), 25402-9.
40. Lai, T. S.; Hausladen, A.; Slaughter, T. F.; Eu, J. P.; Stamler, J. S.; Greenberg, C. S., Calcium regulates S-nitrosylation, denitrosylation, and activity of tissue transglutaminase. *Biochemistry* **2001,** 40, (16), 4904-10.
41. Jin, X.; Stamnaes, J.; Klock, C.; DiRaimondo, T. R.; Sollid, L. M.; Khosla, C., Activation of extracellular transglutaminase 2 by thioredoxin. *The Journal of biological chemistry* **2011,** 286, (43), 37866-73.
42. Fusi, E.; Baldi, A.; Cheli, F.; Rebucci, R.; Ayuso, E.; Sejrsen, K.; Purup, S., Effects of putrescine, cadaverine, spermine, spermidine and β-phenylethylamine on cultured bovine mammary epithelial cells. *Italian Journal of Animal Science* **2008,** 7, (2), 131-140.

Table of Contents graphic